Rapid coupling of Surface Plasmon Resonance (SPR and SPRi) and ProteinChip[TM] based mass spectrometry for the identification of proteins in nucleoprotein interactions

Emeline Bouffartigues[1], Hervé Leh[1], Marielle Anger-Leroy[2], Sylvie Rimsky[1] and Malcolm Buckle[1],*

[1]Enzymologie et cinétique structurale, Laboratoire de Biotechnologies et de Pharmacologie génétique Appliquée, UMR 8113 CNRS, Institut d'Alembert, Ecole Normale Supérieur de Cachan. 61 Ave. du Président Wilson F-94235 Cachan and [2]GenOptics SA Centre Scientifique, Plateau du Moulon, Bâtiment 503, F-91403 Orsay, France

ABSTRACT

We compared coupling approaches of SPR to LC-MS and ProteinChip[TM]-based mass spectrometry (SELDI[TM]) as a means of identifying proteins captured on DNA surfaces. The approach we outline has the potential to allow multiple, quantitative analysis of macromolecular interactions followed by rapid mass spectrometry identification of retained material.

INTRODUCTION

Coupling of quantitative macromolecular analysis techniques such as surface plasmon resonance (SPR) to downstream detection methods and in particular mass spectrometry has become a much sought after goal in proteomics. SPR is a method of choice for interaction analysis since it does away with the necessity of labelling components of an interaction and lends itself to reasonably accurate quantification. However, when complex mixtures are being analysed it is difficult to know which of the components present are actually interacting. In this case, recovery of material from the surface and identification by mass spectrometry provides a powerful means of identification. One of the most widely used SPR technologies is that afforded by the BIAcore optical Bio-sensor platform (1–4), where up to four surfaces may be analysed in series. Coupling between SPR devices and downstream mass spectrometers (BIA/MS) has been investigated for some time (5–7). In practice one can either recover material from the surface (8–10) or directly address the surface retained material and then carry out the analysis by mass spectrometry (11). In the currently available option real-time SPR analysis cannot be carried out with recovery and mass spectroscopy analysis simultaneously due to the configuration of the BIAcore Surface Prep unit. This restriction was addressed by direct coupling of the integrated fluidic cartridge (IFC) of the BIAcore to a HPLC system that itself was linked to an electrospray mass spectrometer (12). However, expansion of this approach for high throughput analysis is severely hampered by the restriction of having only four surfaces available. Finally, a potentially restrictive feature of the BIAcore surfaces is that they rely on immobilization on dextran matrices that can act as non-selective retention supports, thus increasing the background level of non-specific material when complex mixtures are involved.

A solution to these problems is provided here by the use of the emerging technology of SPR imaging (SPRi) coupled to a material recovery protocol and direct analysis by ProteinChip[TM] (SELDI[TM]) mass spectroscopy. The biosensor surfaces developed by GenOptics for use with SPRi consist of prisms made of a high refractive index material with one surface coated with a thin layer of gold. An evanescent field called a plasmon wave is created at the interface of this gold-coated surface and the dielectric from a light beam arriving through the prism at an angle of total internal reflection. At this angle there is a resonance effect that is measured by imaging the entire reflected light from a monochromatic polarized electroluminescent diode using a 10 bit CCD camera linked via a dedicated optical system. Consequently this allows analysis of an entire surface upon which discrete spots of ligand have been immobilized. A microcuvette system allows material to be flowed across the surface and the SPR response at predetermined spots can be assessed in parallel by time resolved CCD that captures changes in percentage reflectivity in the selected spot. Analysis of changes in percentage

*To whom correspondence should be addressed. Tel: +33-147407673; Fax: +33-147407684; Email: buckle@lbpa.ens-cachan.fr

reflectivity averaged across the surface of each spot can then be carried out as a function of time. This can be related to changes in concentration of mass at each spot, thus providing information of the kinetics of the interaction at the surface. In the configuration of SPRi used in these studies we used 16 spots, however in a recent study involving this technology for studying nucleoprotein complexes 25 spots were used (13) and this could, in principle, be extended easily to 400 with no modification of the protocol.

As outlined earlier an advantage of using SPR to visualize interactions is that once material has been seen to be selectively retained at a surface one can then recover the material for analysis by downstream technologies such as mass spectrometry. The ProteinChip^{TM} technology developed by Ciphergen is based on the use of specific surfaces which can be used for the retention of molecules according to affinity or some physical chemical property such as charge, hydrophobicity, etc. (12). Co-crystallization of matrix molecules on these surfaces following selective retention allows mass charge analysis by a matrix-assisted laser desorption ionization (MALDI) mass spectrometer in a process referred to in this context as SELDI^{TM}. Amongst the advantages offered by this approach are the possibilities of using retention chromatography directly coupled to mass spectrometry. We therefore decided to explore the possibility of using the SELDI^{TM} process to analyse material that is selectively retained by SPRi. We compare the approach to a direct online coupling between BIAcore^{TM} and LC-MS.

The nucleoprotein complex we have used in these pilot studies involves the bacterial nucleoid protein H-NS, an atypical global regulator involved in the expression of genes which share the common property of being involved in the bacteria's response to changes in the external environment. A number of H-NS responsive promoters have been shown to contain regions of intrinsic DNA curvature located either upstream or downstream of the transcription start point (14–20). Crucial questions include the nature of the nucleoprotein complexes involving H-NS, and also what other proteins are involved in specific physiological contexts. A working model for H-NS binding has been proposed invoking differential binding to relatively high and low-affinity sites (21). Consequently we decided to determine if we could observe, using SPRi, differential H-NS binding to immobilized DNA containing high and low-affinity sites, and then recover and identify H-NS by mass spectrometry. Since the methodology of SPRi is relatively new, we also compared binding data obtained from SPRi and BIAcore platforms using a sequence-specific DNA-binding protein Integration Host Factor (IHF) (22). The choice of H-NS, however, is primarily dictated by our interest in ultimately identifying proteins that are associated with H-NS in higher order bacterial nucleoid structures. The methodology demonstrated here, i.e. the recovery and subsequent identification of H-NS binding to high-affinity sites, is a prerequisite to demonstrate the feasibility of this approach, and will serve as a basis to recover and identify multiple components of nucleoprotein complexes.

MATERIALS AND METHODS

DNA fragments

The DNA fragments used in this study were PCR products of varying length and composition. For H-NS, two of these sequences are PCR products of DNA sequences inserted upstream of *Escherichia coli gal* minimal promoter (21): (i) a 75-bp curved sequence previously designed to possess a very high degree of intrinsic planar curvature, and consisting of three 21 mers composed of tracts of five and six adenines alternatively repeated (23), (the final fragment will be referred to as 5A6A, total length 223 bp), (ii) a non-curved sequence (88 bp) (referred to as 1A, total length 220 bp), harbouring eight tracts of AGGA motif repeated every 10 bp, designed to be linear possessing no intrinsic curvature. A third fragment is a PCR product of a natural promoter region, i.e. the promoter of *E. coli proU* operon, a 372-bp fragment containing a 200-bp region known to bind H-NS specifically.

Finally, for IHF we used a single 5′biotinylated DNA fragment (205 bp) obtained by PCR amplification of the paca236 fragment (−171 ± 65) between *Eco*RI and *Hind*III containing a single site for binding of the IHF protein (24).

Protein purification

The H-NS protein was purified as described in (25). IHF was prepared as described in (26). CRP was a kind gift of Dr Annie Kolb.

SPR measurements using a BIAcore 2000^{TM} (BIAcore)

H-NS: The 223-bp fragment of DNA 5A6A sequences and one 5′ terminal biotin was passed at 20 µl/min in Hepes buffer (20 mM Hepes pH 7.5, 100 mM NaCl) across a CM5 BIAcore surface to which streptavidin had been previously covalently immobilized. The surface was washed by a short injection of 1 M NaCl (10 µl) to remove non-specifically adsorbed DNA. Various concentrations of H-NS protein in binding buffer (40 mM HEPES pH 8, 8 mM magnesium aspartate, 60 mM potassium glutamate, 1 mM DTT, 0.05% P20) were then passed across the surface at 20 µl/min. At the end of each interaction the surfaces were regenerated by the injection of 1 M NaCl (10 µl).

IHF: The 205 single-end biotinylated fragment containing the IHF site was passed at immobilized to a CM5 surface as for the H-NS fragment immobilization. Various concentrations of IHF were flowed at 20 µl/min across the surface in binding buffer (50 mM sodium cacodylate (pH 7.4), 0.5 mM EDTA 70 mM KCl, 0.05% P20). At the end of each interaction the surfaces were regenerated by the injection of 1 M NaCl (10 µl).

Protein recovery from the BIAcore 2000^{TM} and LC-MS measurements

Samples were recovered from the surface of the BIAcore chips by simply attaching a small-bore tube directly to the exit chamber of the integrated flow cell (IFC) of the BIAcore 2000 that was then connected through a switch to

a reverse phase column on an HPLC (ETTAN[TM], Amersham-Pharmacia). H-NS (500 nM) was flowed across a surface containing immobilized 5A6A DNA fragment and at equilibrium binding buffer alone was allowed to pass across. After a length of time equivalent to 1.5 times the dead volume (i.e. the volume between the surface and the collecting column, estimated as being 100 μl) all non-retained H-NS was assumed to have passed across the surface and any H-NS present must constitute H-NS retained by the DNA. The bound H-NS was eluted from the surface by the injection of 10 μl of 1 M NaCl and the elution passed directly across a MAGIC C18 5 μm 200 Å column (Michron BioResources). The column was washed with 2% acetonitrile 0.1% acetic acid, and then material eluted directly online into an ETTAN[TM] Electrospray (Amersham Pharmacia-Analytica of Branford, USA) using a solution of 70% acetonitrile and 0.1% acetic acid. Deconvolution of electrospray mass spectrograms was facilitated by the use of the MagTran deconvolution programme.

SPRi measurements using an SPRi–Plex[TM] (GenOptics)

The reactive surface for the SPRi measurements consists of a gold surface coated prism treated with 11-mercaptoundecanoic acid (MUA) coupled to a layer of poly(ethylenimine) to which extravidin is covalently attached (27). Biotinylated DNA probes may then be attached through the biotin–extravidin interaction. We immobilized singly 5′-end labelled DNA fragments containing the *proU*, 5A6A and 1A sequences to the prism surfaces by direct spotting of ~100 nl of 10 μg/ml (~50 nM) solutions of each DNA fragment. The surfaces were allowed to dry and were then mounted in the *SPRi–Plex*[TM] apparatus and washed by a short (10 μl) injection of 1 M NaCl followed by continuous flow (50 μl/min) with binding buffer. The spots containing DNA were visually identified by the relative change in percent reflectivity and delineated in the accompanying software as circles on the image. Various concentrations of protein were injected across the surface in binding buffer at 50 μl/min. Images were recorded at a rate of 1 Hz and the rate of change of percent reflectivity across the area of each predetermined spot used to calculate the kinetics of change in binding at the surface.

Protein recovery from the SPRi–Plex[TM] and SELDI[TM] measurements

The surface was treated with an injection of 10 μl of NaCl (1 M) at 50 μl/min which effectively removed bound H-NS. H-NS (250 nM) was then reinjected at 50 μl/min and after 2 min into the dissociation phase the flow was stopped, the surface removed from the apparatus and air dried. Each spot was treated by the addition of 1 μl of NaCl (1 M). The spots were allowed to sit for 30 s then the solutions recovered and spotted onto a ProteinChip[TM] H50 hydrophobic surface and left to incubate for 60 min in a humid chamber to avoid evaporation. Excess liquid was removed from each of the spots which were then washed by the 2-fold addition of 1 μl of distilled water.

The spots were then dried; co-crystallized with 1 μl of a 20% solution of matrix and read in a SELDI[TM] ProteinChip reader.

RESULTS AND DISCUSSION

Relative comparison of binding using the BIAcore and *SPRi–Plex*[TM] approaches

The SPR approach consists of immobilizing ligands to a surface and then observing changes in the refractive index at the surface as molecules bind. We compare two applications that use this technology. The first involves a BIAcore 2000[TM] based approach where a solution flows through a microfluidic interface across four dextran coated (~100 nm thick) gold surfaces on a biosensor chip. Changes in surface plasmon resonance on the surface are reported as changes in the angle at which the intensity of the reflected light decreases. Empirically in the BIAcore technology 1 ng of a globular protein or 0.78 ng of a DNA molecule bound at the surface gives a response of 1000 Resonance Units (RU) (3).

We immobilized 142 RU of the 223-bp 5A6A DNA fragment to a carboxymethylated dextran surface. Thus we can expect ~0.1 ng or 7×10^{-16} mol or 4×10^{8} molecules of DNA distributed within the dextran layer. Due to the nature of the surface we can make no assumptions concerning the distribution of the DNA molecules or their orientation within this dextran layer.

We then passed concentrations of H-NS across this surface to obtain sensorgrams such as those shown in Figure 1A. In classical Langmuir type situations the apparent dissociation rate constant k_d may be obtained by fitting the dissociation phase to a simple exponential expression where the relative change in resonance response (R) as a function of time (t) with respect to R at time $t = 0$, ($R_{(0)}$), results from $R_{(t)} = R_{(o)} \cdot \exp^{(-kd \cdot t)}$ and the apparent association rate constant k_a is obtained from $R_{(t)} = R_{(max)} \cdot (1 - \exp^{(-(ka \cdot C + kd) \cdot t)})$ at a given protein concentration of (C), where $R_{(max)}$ is the response at steady state. Only in the case of the 5A6A fragment which contained a high-affinity binding site could we obtain single site binding affinity curves. From these we calculated apparent kinetic constants some of which are shown for the concentration of 250 nM H-NS in Table 1. Under these conditions we could estimate the amount of H-NS bound to the DNA at saturation as being ~159 RU thus 0.16 ng, 10^{-14} mol or 0.6×10^{10} molecules of H-NS. Since 4×10^{8} molecules of DNA were calculated as being present at the surface, the stoichiometry of binding was thus ~14 molecules of H-NS monomers/molecule of DNA.

We then used the *SPRi–Plex*[TM] machine developed by GenOptics in which a microcuvette, in contact with a sensor surface, is used to introduce macromolecules by continuous flow to ligands immobilized on the sensor surface. The sensor surface consists of a gold-coated prism treated with a layer of 11-MUA, poly(ethylenimine) (PEI) and finally with extravidin. Biotinylated molecules may be attached to the surface as a monolayer through the strong interaction with extravidin. We immobilized
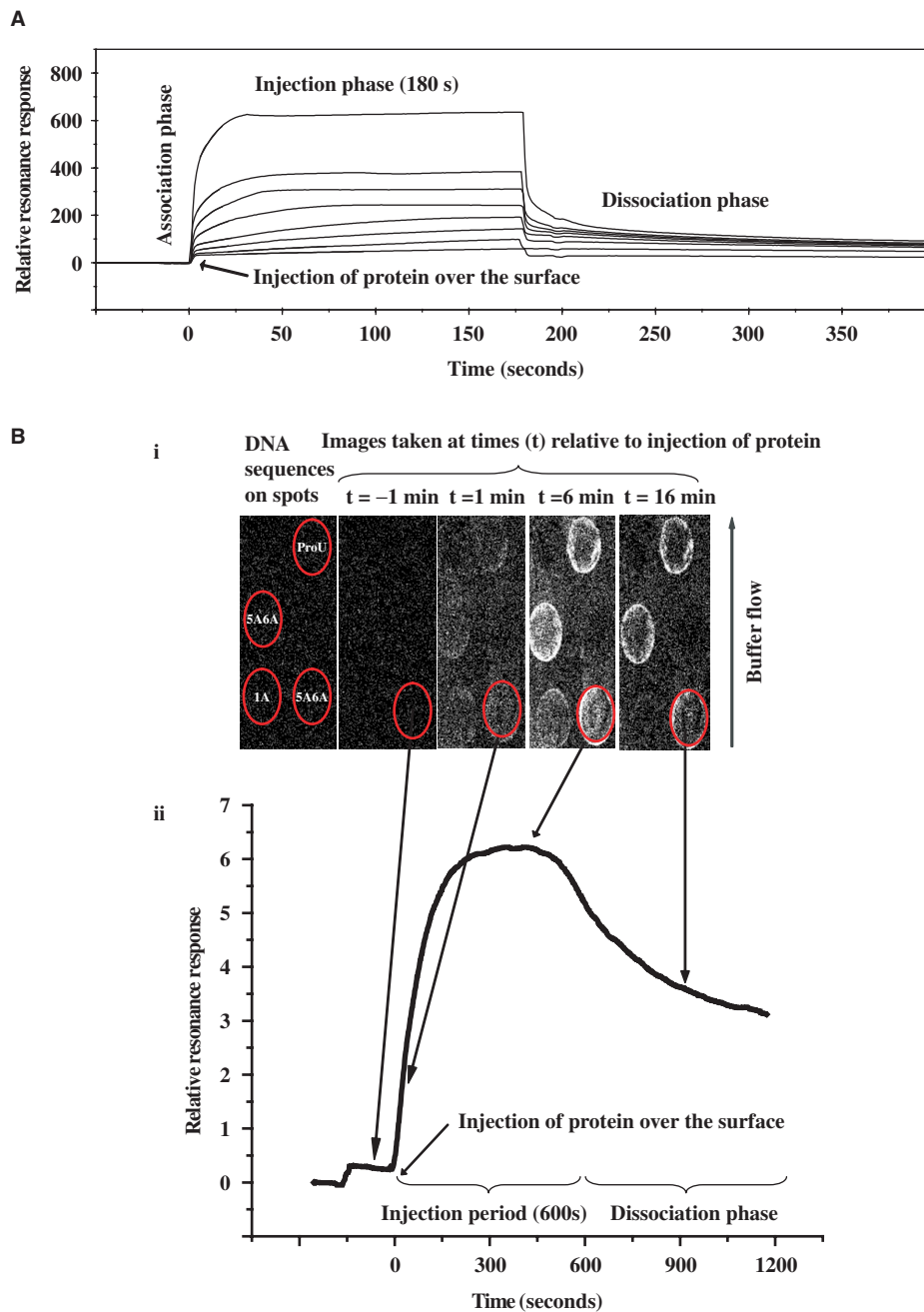
Figure 1. Surface plasmon resonance measurements for H-NS binding to DNA fragments immobilized on a surface. (**A**) SPR measurements on surfaces containing immobilized 5A6A DNA fragments were carried out on a BIAcore 2000™ as described in Materials and Methods section. Sensorgrams are shown of H-NS at various concentrations (20–600 nM) flowing across the 5A6A surface. (**B**) SPRi measurements on surfaces containing immobilized 5A6A DNA fragments. (i) Images of the prism surface of the *SPRi–Plex*™ SPR device (GenOptics) containing immobilized DNA fragments. The spots have been circled in this representation with the name of the respective DNA fragment in each circle. The DNA was applied at a concentration of 10 μg/ml (∼50 nM) for all fragments. Each spot has a surface area of ∼0.78 mm². H-NS (500 μl of 500 nM) was flowed across the surface at 50 μl/min (thus contact time = 10 min) in binding buffer. (ii) Kinetic curve of the binding of H-NS (500 nM) to the prism surface. Images were taken at 1 s intervals and the relative change in resonance response plotted as a function of time of injection. The arrows show the image associated with a specific time point on the curve.

three different DNA fragments containing the *proU*, 5A6A and 1A sequences to pre-treated extravidin sensor surfaces. A section of the surface is shown in Figure 1B (i) in which 0.5 μl of 5A6A is spotted at 10 μg/ml (0.5 μM) duplicate, the *proU* fragment (10 μg/ml 0.5 μM) and 1A fragment (10 μg/ml 0.5 μM) are spotted alone. Each spot was pre-chosen using the inherent

software that allowed an area of increased reflectivity to be delineated. The percentage reflectivity (R_{2TM}) averaged across a spot at a given time is calculated from the expression

$$R_{2TM} = \frac{(Niv_{TM} - Niv_0)\, R_{2TE}\, T_{1TE}^2}{(Niv_{TE} - Niv_0)\, T_{1TM}^2}$$

Table 1. Apparent kinetic parameters for H-NS binding to the immobilized DNA fragment containing the 5A6A sequence

SPRi–Plex	k_d (s^{-1})	k_a (M^{-1}s^{-1})	K_d (M^{-1})
H-NS (250 nM)	3.0×10^{-3}	1.1×10^5	2.8×10^{-8}
H-NS (250 nM)	5.0×10^{-3}	1.4×10^5	3.5×10^{-8}
H-NS (250 nM)	3.6×10^{-3}	0.7×10^5	5.1×10^{-8}
Average	$3.9 \pm 1 \times 10^{-3}$	$1.1 \pm 0.3 \times 10^5$	3.7×10^{-8}
Biacore 2000			
H-NS (250 nM)	2.9×10^{-3}	0.8×10^5	3.6×10^{-8}
H-NS (250 nM)	2.9×10^{-3}	1.1×10^5	2.8×10^{-8}
H-NS (250 nM)	3.2×10^{-3}	1.8×10^5	1.8×10^{-8}
Average	$3.0 \pm 0.1 \times 10^{-3}$	$1.2 \pm 0.5 \times 10^5$	2.7×10^{-8}

Note: SPR measurements were carried out on DNA fragments immobilized through a biotin/streptavidin interaction at either a Biacore SPR sensorchip surface or a GenOptics *SPRi–Plex* prism surface. H-NS (250 nM) was flowed across the respective surfaces as described in Materials and Methods section to generate curves of the type shown in Figure 1. The resulting data were analysed using the Origin Pro fitting programme to obtain apparent dissociation (k_d) and association (k_a) values. The experiment was repeated $3\times$ at the same concentration at each surface. Average values and standard deviation for k_d, k_a and K_d were derived from the three results obtained at 250 nM H-NS for each instrument. SPR measurements at the Biacore surface over a range from 20 to 600 nM H-NS were also carried out (data not shown) and allowed the construction of a Langmuir binding isotherm from which an apparent K_d of 3.0×10^{-8} M could be calculated.

where Niv is the grey level pixel density across a single spot, the polarization of electromagnetic radiation measured in a plane perpendicular to the propagation direction of the beam is either TE (or s) having no electric field in the incidence plane or TM (or p) having no magnetic field in the incidence plane. Thus Niv$_0$ is the background level, and Niv$_{TE}$ and Niv$_{TM}$ are the pixel densities measured at the two respective polarization modes. T_1 is the transmission coefficient of the intensity at the prism entry and R is the reflection coefficient of intensity at the gold-coated surface of the prism. Thus effectively three measurements are made, Niv$_0$ the background noise; (Niv$_{TE} - N$iv$_0$) which is the measure of the TE signal and (Niv$_{TM} - N$iv$_0$) the measure of the TM signal. This then allows an estimation of the apparent density of material (Γ in pg/mm^2) on the surface for each spot using the expression

$$\Gamma = \frac{|n_c - n_b| \cdot d_b}{\delta n / \delta C}$$

where n_c is the refractive index of the surface layer; n_b is the refractive index of the biological molecules, d_b is the geometric thickness of the biological medium and $\delta n/\delta C$ is the dependence of the variation in biological medium refractive index as a function of concentration. This leads to

$$\Gamma = \frac{\Delta R \cdot L_{zc}}{S_{P,R} \cdot \delta n / \delta C}$$

where ΔR is the variation of reflectivity (expressed as%) and ($S_{P,R}$) the variation of reflectivity per unit of variation of refractive index ($\partial R/\partial n$) is calibrated for the apparatus used based on measurements of the variation in reflectivity between two solutions having closely related refractive

indexes (in this case 2.25×10^{-3}); the penetration depth of the evanescent wave in the medium immediately above the gold layer (L_{zc}) is 1.02×10^{-4} mm, and $\delta n/\delta C$ for proteins and nucleic acids is 1.9×10^{-10} mm^3/pg.

It is clear from inspection of the images that the current state of the art of spotting DNA onto the surface is not optimal, the uniformity of the surface is still difficult to control and replicate spots had a variability of up to 20% in the amount of material bound to the surface. However, typical values based on Γ measurements gave $\sim$69 fmol/mm^2 for 5A6A containing fragments; thus on a surface area of $\sim$0.78 mm^2 this gave a total of $\sim$44 fmol, or 3×10^{10} molecules of DNA. There are no data that suggest that the DNA is in fact arranged perpendicular to the surface and indeed the presence of extravidin may indeed aid the DNA to compact and collapse on the surface, however assuming that this is not the case then these values suggest that the average distance in this case between each DNA fragment would be about 10 nm. A similar calculation for the three fragments at the different surfaces provided similar values for immobilization of the fragments. Note that there is no indication of the distribution of immobilized DNA in the dextran layer on the BIAcore nor would there be any way of calculating its distribution even were a simple gold surface used.

At time $t = 0$ s, a solution of H-NS (250 nM) was injected at 50 µl/min through the microcuvette and an image recorded every second during the association and dissociation phases [Figure 1B (i)]. All the regions on the surface containing DNA were seen to react, to different degrees, with the protein flowing across the surface. A more intense interaction at the perimeters of each spot is due to a concentration of DNA during the immobilization process. During the dissociation phase protein rapidly dissociated from the DNA surfaces containing the 1A fragment. Kinetic curves based on the relative change in resonance response (in fact of percent reflectivity of the surface of each spot as described earlier) as a function of time were assembled from the images [Figure 1B (ii)]. As for the BIAcore analysis a single binding site model for the 5A6A containing fragment allowed calculation of apparent rate constants (Table 1) and of an equilibrium dissociation constants (K_d) for the 5A6A fragment reaction of 3.7×10^{-8} M that were similar to those calculated on the BIAcore surfaces. We were able to calculate from images of the surfaces at saturation that $\sim$360 fmol of H-NS were bound to the 5A6A fragment containing surface; thus giving a stoichiometry of $\sim$8 monomers of H-NS per DNA fragment molecule. Surfaces were regenerated by injecting a solution of 20 µl of NaCl (1 M) into the microcuvette; this effectively removed the protein but did not alter the amount of DNA bound to the surface. The image at $t = -1$ min in Figure 1B (i) represents an image of a surface subsequent to NaCl regeneration prior to re-injection of the protein.

Figure 1B clearly demonstrates a differential binding of H-NS to *proU* and the 5A6A fragments. On the other hand, H-NS bound but rapidly dissociated from the fragments of DNA containing the 1A sequence. This observation and the values for the relative affinities of binding whether obtained from BIAcore or SPRi

approaches are in good agreement with previous observations made on the relative binding of H-NS to these fragments of DNA (21), where H-NS binding constants in the order of 30 nM were obtained for H-NS binding to DNA containing 5A6A fragments. No H-NS binding was observed to any part of the surface not containing immobilized DNA.

The stoichiometry of binding was estimated as being 8 monomers of H-NS per DNA on the 5A6A fragments and 22 monomers of H-NS per DNA of *proU* fragments. There is intrinsically a degree of error in estimating the concentration of DNA on the surface. However, these values do not differ dramatically from those observed on the BIAcore experiments.

Since H-NS is generally perceived to bind in a sequence non-specific manner with a preference for bent DNA, we decided to look at the binding of transcription factors that bound to single or multiple high-specificity sites on DNA. First we looked at the binding of the cyclic AMP binding protein (CRP) in the presence of cAMP to fragments of DNA containing the *lac* promoter and a CRP binding site. In the BIAcore configuration we could get specific binding only in the presence of very high BSA concentrations and under no conditions could we distinguish the association phase from interactions between CRP–cAMP and the streptavidin surface. Indeed when we looked at the interaction using the *SPRi–Plex*™ surfaces we could only distinguish the dissociation phase when non-specific binding had decreased sufficiently to reveal images of CRP selectively retained at the surface. Consequently we were unable to find conditions where we could compare specific binding of cAMP–CRP to DNA immobilized at an SPR surface.

IHF is a heterodimeric *E. coli* protein that binds several specific DNA sequences in the bacterial genome (22). We immobilized DNA fragments containing a single IHF binding site to both BIAcore and *SPRi–Plex* surfaces and analysed binding of IHF in both instruments to obtain apparent binding constants which are shown in Table 2. Essentially the kinetic parameters of binding of IHF to immobilized DNA were the same, independent of the surface or the SPR technology used, in agreement with what we observed with H-NS. These values are in full agreement with those in the literature (22). Both BIAcore and *SPRi–Plex* techniques allowed rapid analysis of binding with single affinities of DNA binding proteins to immobilized DNA.

Recovery of material from SPR and SPRi surfaces for mass spectrometry analysis

A fresh BIAcore sensorchip surface was prepared of immobilized DNA containing the 5A6A fragment and H-NS (500 nM) passed across the BIAcore apparatus. Approximately 292 RU of H-NS, equivalent to 0.3 ng or 2×10^{-14} moles, were bound to the surface. At the onset of the dissociation phase, NaCl was injected as described in Materials and Methods section in order to selectively remove the retained H-NS from the DNA. The material was collected on a reverse phase column, desalted and analysed directly on line by an electrospray mass

Table 2. Apparent kinetic parameters for IHF binding to immobilized DNA fragments on Biacore and SPRi–Plex surfaces

Technique	k_d (s^{-1})	k_a (M^{-1}s^{-1})	K_d (M^{-1})
Biacore	$4.8 \pm 3.0 \times 10^{-3}$	$1.7 \pm 0.9 \times 10^5$	$2.6 \pm 0.3 \times 10^{-8}$
SPRi–Plex	$3.1 \pm 0.5 \times 10^{-3}$	$1.6 \pm 0.4 \times 10^5$	$2.0 \pm 0.7 \times 10^{-8}$

Note: SPR measurements were carried out on DNA fragments containing a single IHF binding site immobilized through a biotin/streptavidin interaction at either a Biacore SPR sensorship surface or a GenOptics *SPRi–Plex* prism surface. IHF was flowed across the respective surfaces. The resulting data were analysed to obtain apparent dissociation (k_d) and association (k_a) values. The experiment was carried out over a range of concentrations from 20 to 180 nM IHF at each surface. The k_a and k_d values were obtained from a fit of each individual experiment; the K_d values were obtained from the ratio of k_d/k_a for each experiment and the values shown are the average for all the values obtained. The same experiments allowed calculation of surface saturation at steady state and thus the construction of a simple Langmuir binding isotherm from which apparent K_d's of 4.2×10^{-8} M for the Biacore and 3.2×10^{-8} M for the SPRi–Plex were calculated.

spectrometer (Analytica of Branford). A mass spectrogram of H-NS injected directly via a C18 column onto the electrospray is shown in Figure 2A. Deconvolution of the m/z spectrum carried out using the MagTran program gave the masses shown in Figure 2B. H-NS has an average mass of 15 539.66 Da; we observed two main peaks having apparent masses of 15 484 and 15 642 Da. The protein consists of a mixture of the N-formylated methionine-containing H-NS, H-NS lacking the N-terminal methionine and an adduct of the protein with β-mercaptoethanol.

The eluted material from the BIAcore gave the spectrum shown in Figure 2C. The majority of the peaks are separated by 44 Da due to the presence of Tween in the elution buffer. Removal of this polymer from the elution protocol invariably causes problems of non-specific binding within the microfluidics. Consequently it is almost impossible to identify m/z values indicative of H-NS alone. In a similar study on a different system, samples were actually fractionated, treated with strong cation exchange ZipTips to remove as much detergent polymer as possible, digested and peptides identified by electrospray (12). This accumulates handling, does not completely alleviate the polymer contamination problem and does not allow unequivocal identification of complex mixtures. Thus, whilst we could elute and partially identify by mass spectrometry whole proteins immobilized on BIAcore sensor surfaces this remained, in our hands, an ambiguous and difficult procedure that was really only feasible following subsequent isolation and digestion of eluting proteins (12). We conclude therefore that modification of the IFC of the BIAcore 2000™ does not allow satisfactory recovery and identification of material following SPR analysis.

We therefore decided to compare a different approach using SPR imaging coupled with SELDI™. As shown earlier DNA fragments could be easily immobilized on a monolayer extravidin SPRi surface using biotinylated end groups. Because of the nature of the surface one can
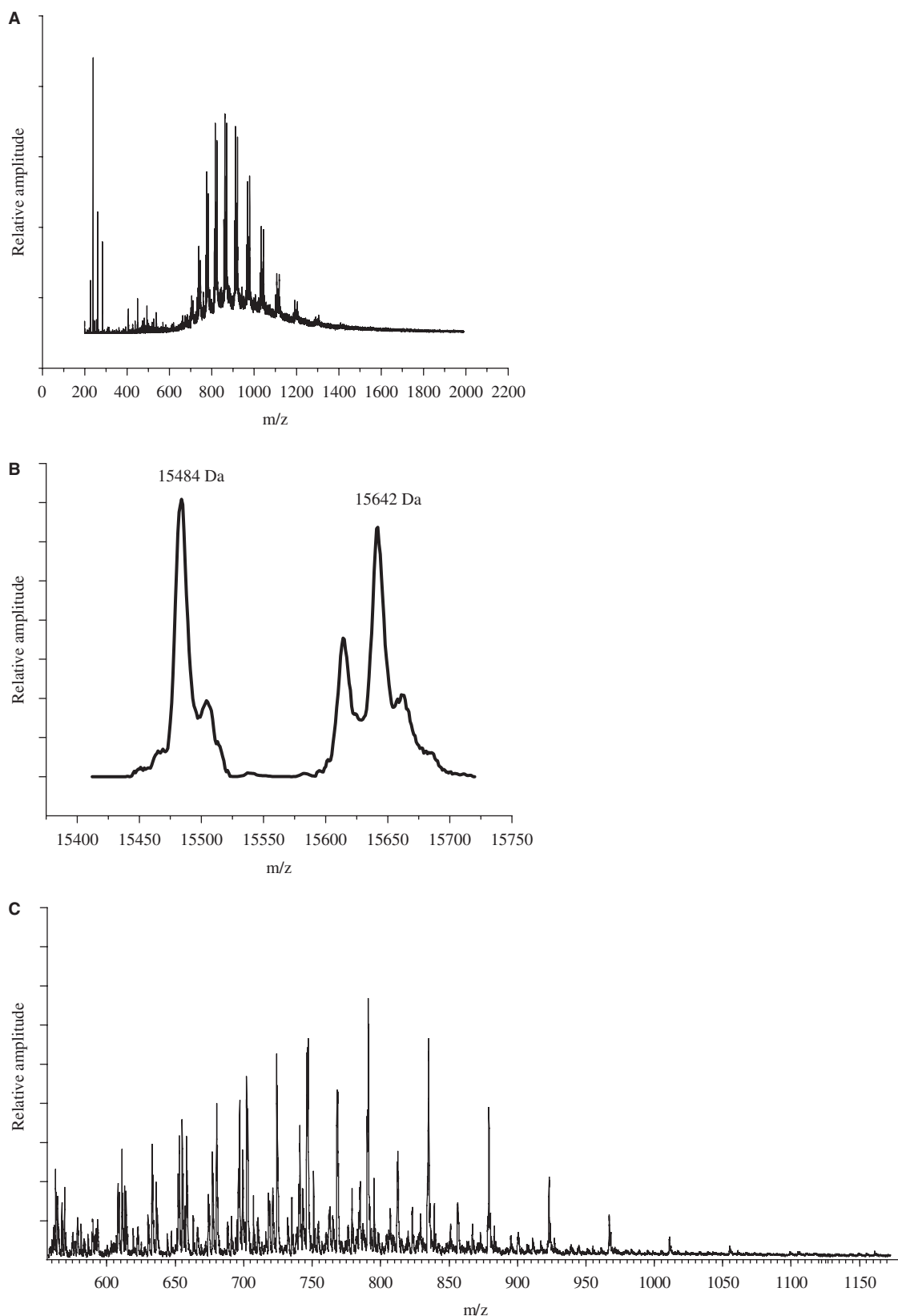
Figure 2. Electrospray spectra of H-NS. H-NS either free in solution or after recovery from a BIAcore surface was injected into an ETTAN electrospray (Analytica of Branford) at a flow rate of 200 μl/min as described in Materials and Methods section. (**A**) Non-deconvoluted spectrum of H-NS prior to injection across the BIAcore surface. (**B**) Resolved spectrum of the spectrum shown in (**A**) identifying two isoforms of H-NS. Masses are expressed as average masses; H-NS has a calculated average mass of 15 539.66 Da (see text for discussion). (**C**) Non-deconvoluted spectrum of material eluted from a BIAcore surface containing immobilized DNA fragments containing the 5A6A sequence.
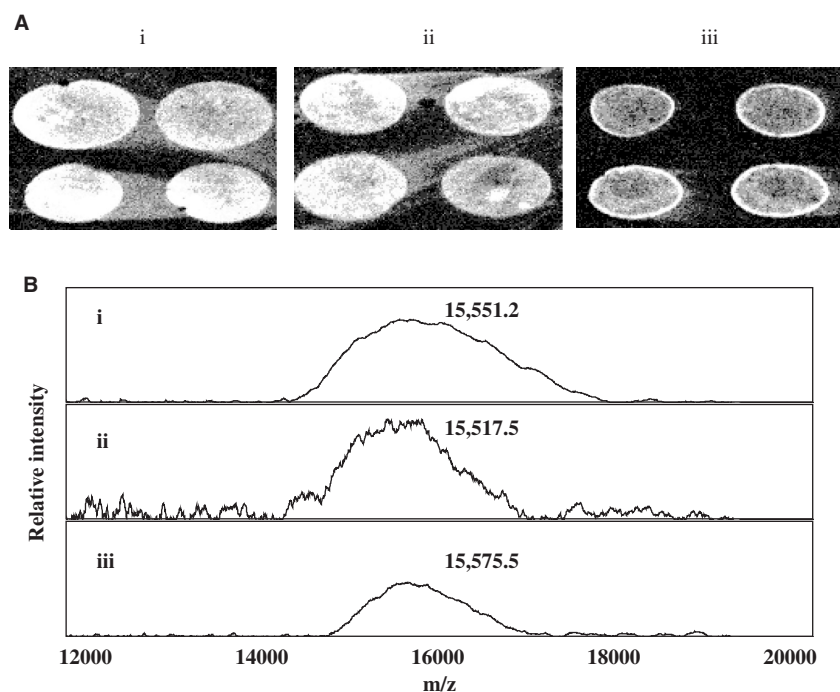
Figure 3. Recovery of material after SPRi for mass spectrometry analysis. (**A**) Images of H-NS retained at a *SPRi–Plex*[TM] prism surface by immobilized DNA. The images were obtained as described in Materials and Methods section. (i) Images of surfaces of immobilized DNA fragments containing the 5A6A sequence, and ensuing mass spectra of material eluted from these surfaces. (ii) Images of surfaces of immobilized DNA fragments containing the *proU* sequence, and ensuing mass spectra of material eluted from these surfaces. (iii) Images of surfaces of immobilized DNA fragments containing the 1A sequence, and ensuing mass spectra of material eluted from these surfaces. (**B**) Mass spectra of proteins removed from this surface, adsorbed onto a H4 ProteinChip[TM] array and read on a ProteinChip reader[TM] (SELDI[TM]). Two minutes after injection of H-NS (500 nM, 500 μl at 50 μl/min) onto the surface, the buffer flow was stopped and the surface removed and air dried. Proteins were then transferred, as described in Materials and Methods section, from four spots corresponding to each DNA sample to an H4 ProteinChip[TM] surface and any material present detected by mass spectrometry. Spectra were obtained under identical conditions of laser intensity, sensitivity and data acquisition. The peak intensity is expressed as a relative value normalized between the spectra and thus the relative area under each peak is representative of the amount of material detected by the spectrometer, *m/z* refers to the mass to charge ratio and the values obtained for each peak represent average mass, the charge is assumed to be +1. (i) Material recovered from the four surfaces in Figure 3A (i) (containing the 5A6A DNA fragment), (ii) material recovered from the four surfaces in Figure 3A (ii) (containing the *proU* DNA fragment) and (iii) material recovered from the four surfaces in Figure 3A (iii) (containing the 1A DNA fragment).

calculate relative densities of binding, around 44 fmol/mm^2, and thus the average distances between DNA fibres which were of the order of 10 nm. These values are in good agreement with those reported by (13) for a similar approach using this technology. The kinetic parameters of binding of H-NS to DNA fragments using this approach was demonstrated earlier to be similar to those derived from analysis using the BIAcore. A surface was prepared using the *SPRi–Plex*[TM] apparatus with the configuration shown in Figure 3A with DNA fragments containing 5A6A [Figure 3A (i)], *proU* [Figure 3A (ii)] and 1A [Figure 3A (iii)], but this time the flow was stopped after 2 min into the dissociation phase. The surface was removed and air dried. The surface was stored at room temperature during transfer to a separate institute. The dried materials on the surfaces were still visible after removal from the apparatus. Each spot was then treated with 1 μl of a solution of NaCl (1 M), the material from four similar spots [e.g. Figure 3A (i)] was pooled and the salt solution transferred to and adsorbed onto a H4 hydrophobic ProteinChip[TM] surface (Ciphergen) which was air dried then washed 3× by the addition and removal of 2 μl of distilled water, then 2 μl of

5% acetonitrile 0.1% trifluoroacetic acid (TFA). The choice of SELDI[TM] is preferred since although in this instance the recovery protocol involved the use of high salt concentrations, in other cases regeneration of the surface could require a variety of conditions encompassing chaotropic reagents (SDS, guanidine HCl, urea, etc.) extremes of pH (glycine pH 3.0, 10 mM NaOH) and specific competitors (antibodies, peptides) and thus the diverse range of different ProteinChip[TM] surfaces available (ion exchange, hydrophobic hydrophilic, affinity, etc.) allows direct spotting of the recovered material onto the requisite ProteinChip[TM] surface without introducing intermediate steps that could lead to dilution, contamination or even loss of material.

The air-dried ProteinChip[TM] surface was then analysed using a SELDI[TM] ProteinChip reader (SELDI[TM]) (Figure 3B). Material from four surfaces was pooled and the amount of H-NS present at the moment of dissociation from the surface containing the 5A6A fragment estimated as being ∼2 pmol/mm^2 equivalent to 1.4 pmol, 22 ng of H-NS or 9×10^{11} molecules on a given surface. A peak of around 15 500 *m/z* was observed in all the spectra of material obtained from the different surfaces.

No peaks were obtained from material eluted from areas of the surface that did not contain DNA (data not shown). Accurate estimation of the mass of proteins eluted from the DNA surfaces is difficult due to the relatively small amounts of material assumed to be present, although an average mass of 15 547 Da was obtained which correlates well with both the expected values for H-NS and with those obtained for H-NS on the SELDI[TM] ProteinChip[TM] reader (data not shown) and H-NS on the electrospray (Figure 2). The relative amount of H-NS bound to 5A6A [Figure 3A (i)] and *proU* [Figure 3A (ii)] compared to that bound to 1A [Figure 3A (iii)] was 2.2 and 2.1 (5A6A:1A and *proU*:1A, respectively); the ratios of the relative areas of the recovered peaks from these surfaces (Figure 3B) was 2.7 and 2.1, respectively, thus there is a clear correlation between the amount of material present on the surface and that recovered and identified by mass spectroscopy. We could observe masses from all the three surfaces studied here (average mass 15 547 Da) that corresponded with that expected for H-NS showing that we were able to recover material from the surface. The transfer protocol thus allowed quantitative recovery of material from the SPRi surfaces to the SELDI ProteinChip[TM] surfaces and detection by mass spectrometry.

We also recovered material from the *SPRi–Plex* surfaces used to investigate IHF binding to immobilized DNA containing a single IHF binding site. We could bind IHF to the immobilized DNA on the surfaces and then elute retained IHF (using 3 μl of 4 M NaCl) and transfer the material to SELDI surfaces. We observed two peaks at $m/z = 10 773$ and 11 354 Da (data not shown) corresponding to the beta (10 651 Da) and alpha (11 354 Da) subunits, respectively of IHF. We noted that although we could quantify the binding interaction involving 1 fmol of IHF to the surface by *SPRi–Plex* we could not obtain m/z spectra from material recovered from these surfaces and needed to increase the amount of retained IHF to at least 1 pmol before obtaining an easily recognizable spectrum. Thus for both IHF and H-NS a minimum of $\sim$1 pmol or $\sim$10^{12} molecules could be visualized after recovery.

We thus demonstrate that monolayer surfaces permit accurate SPR analysis of macromolecular interactions and that the *SPRi–Plex*[TM] configuration is well suited to a simple recovery protocol that provides rapid sensitive mass spectrometry analysis. Clearly at these levels of surface saturation more than 100 spots could be rapidly visualized and the material recovered for analysis by SELDI even with the manual approach used here. An important question relates to the actual protein composition of nucleoprotein complexes containing H-NS since a reasonable structure exists only for separate domains of H-NS (18,28,29), and little is known how it interacts with other structural proteins (FIS, HU, CRP, IHF, etc.) in the bacterial chromatin. We are therefore currently applying this approach to investigating complex mixtures retained at specific DNA surfaces as well as automating the process for high fidelity reproducible high throughput.

REFERENCES

1. Fagerstam,L.G., Frostell,A., Karlsson,R., Kullman,M., Larsson,A., Malmqvist,M. and Butt,H. (1990) Detection of antigen-antibody interactions by surface plasmon resonance. Application to epitope mapping. *J. Mol. Recognit.*, **3**, 208–214.
2. Malmqvist,M. (1993) Biospecific interaction analysis using biosensor technology. *Nature*, **361**, 186–187.
3. Buckle,M., Williams,R.M., Negroni,M. and Buc,H. (1996) Real time measurements of elongation by a reverse transcriptase using surface plasmon resonance. *Proc. Natl. Acad. Sci. U.S.A.*, **93**, 889–894.
4. Rimsky,S. and Buckle,M. (2004). Protein-DNA interactions. In Meyers,RA (ed), *Encyclopedia of Molecular Cell Biology and Molecular Medicine*. **Wiley-VCH**, Vol. 3.
5. Nedelkov,D. and Nelson,R.W. (2003) Surface plasmon resonance mass spectrometry: recent progress and outlooks. *Trends Biotechnol.*, **21**, 301–305.
6. Nedelkov,D. and Nelson,R.W. (2003) Design and use of multi-affinity surfaces in biomolecular interaction analysis-mass spectrometry (BIA/MS): a step toward the design of SPR/MS arrays. *J. Mol. Recognit.*, **16**, 15–19.
7. Nedelkov,D. and Nelson,R.W. (2003) Delineating protein-protein interactions via biomolecular interaction analysis-mass spectro-metry. *J. Mol. Recognit.*, **16**, 9–14.
8. Sonksen,C.P., Nordhoff,E., Jansson,O., Malmqvist,M. and Roepstorff,P. (1998) Combining MALDI mass spectrometry and biomolecular interaction analysis using a biomolecular interaction analysis instrument. *Anal. Chem.*, **70**, 2731–2736.
9. Lopez,F., Pichereaux,C., Burlet-Schiltz,O., Pradayrol,L., Monsarrat,B. and Esteve,J.P. (2003) Improved sensitivity of biomolecular interaction analysis mass spectrometry for the identification of interacting molecules. *Proteomics*, **3**, 402–412.
10. Zhukov,A., Schurenberg,M., Jansson,O., Areskoug,D. and Buijs,J. (2004) Integration of surface plasmon resonance with mass spectrometry: automated ligand fishing and sample preparation for MALDI MS using a Biacore 3000 biosensor. *J. Biomol. Tech.*, **15**, 112–119.
11. Krone,J.R., Nelson,R.W., Dogruel,D., Williams,P. and Granzow,R. (1997) BIA/MS: interfacing biomolecular interaction analysis with mass spectrometry. *Anal. Biochem.*, **244**, 124–132.
12. Font,M.P., Cubizolles,M., Dombret,H., Cazes,L., Brenac,V., Sigaux,F. and Buckle,M. (2004) Repression of transcription at the human T-cell receptor V beta 2.2 segment is mediated by a MAX/MAD/mSin3 complex acting as a scaffold for HDAC activity. *Biochem. Biophys. Res. Commun.*, **325**, 1021–1029.
13. Maillart,E., Brengel-Pesce,K., Capela,D., Roget,A., Livache,T., Canva,M., Levy,Y. and Soussi,T. (2004) Versatile analysis of multiple macromolecular interactions by SPR imaging: application to p53 and DNA interaction. *Oncogene*, **23**, 5543–5550.
14. Spurio,R., Falconi,M., Brandi,A., Pon,C.L. and Gualerzi,C.O. (1997) The oligomeric structure of nucleoid protein H-NS is necessary for recognition of intrinsically curved DNA and for DNA bending. *EMBO J.*, **16**, 1795–1805.
15. Ueguchi,C. and Mizuno,T. (1996) Purification of H-NS protein and its regulatory effect on transcription in vitro. *Methods Enzymol.*, **274**, 271–276.

16. Zhang,A., Rimsky,S., Reaban,M.E., Buc,H. and Belfort,M. (1996) Escherichia coli protein analogs StpA and H-NS: regulatory loops, similar and disparate effects on nucleic acid dynamics. *EMBO J.*, **15**, 1340–1349.
17. Schroder,O. and Wagner,R. (2002) The bacterial regulatory protein H-NS–a versatile modulator of nucleic acid structures. *Biol. Chem.*, **383**, 945–960.
18. Shindo,H., Ohnuki,A., Ginba,H., Katoh,E., Ueguchi,C., Mizuno,T. and Yamazaki,T. (1999) Identification of the DNA binding surface of H-NS protein from Escherichia coli by heteronuclear NMR spectroscopy. *FEBS Lett.*, **455**, 63–69.
19. Ueguchi,C., Seto,C., Suzuki,T. and Mizuno,T. (1997) Clarification of the dimerization domain and its functional significance for the Escherichia coli nucleoid protein H-NS. *J. Mol. Biol.*, **274**, 145–151.
20. Ueguchi,C. and Mizuno,T. (1993) The Escherichia coli nucleoid protein H-NS functions directly as a transcriptional repressor. *EMBO J.*, **12**, 1039–1046.
21. Rimsky,S., Zuber,F., Buckle,M. and Buc,H. (2001) A molecular mechanism for the repression of transcription by the H-NS protein. *Mol. Microbiol.*, **42**, 1311–1323.
22. Dhavan,G.M., Crothers,D.M., Chance,M.R. and Brenowitz,M. (2002) Concerted binding and bending of DNA by Escherichia coli integration host factor. *J. Mol. Biol.*, **315**, 1027–1037.
23. Ulanovsky,L., Bodner,M., Trifonov,E.N. and Choder,M. (1986) Curved DNA: design, synthesis, and circularization. *Proc. Natl. Acad. Sci. U.S.A.*, **83**, 862–866.
24. Browning,D.F., Beatty,C.M., Sanstad,E.A., Gunn,K.E., Busby,S.J. and Wolfe,A.J. (2004) Modulation of CRP-dependent transcription at the Escherichia coli acsP2 promoter by nucleoprotein complexes: anti-activation by the nucleoid proteins FIS and IHF. *Mol. Microbiol.*, **51**, 241–254.
25. Tanaka,K., Muramatsu,S., Yamada,H. and Mizuno,T. (1991) Systematic characterization of curved DNA segments randomly cloned from *Escherichia coli* and their functional significance. *Mol. Gen. Genet.*, **226**, 367–376.
26. Nash,H.A., Robertson,C.A., Flamm,E., Weisberg,R.A. and Miller,H.I. (1987) Overproduction of Escherichia coli integration host factor, a protein with nonidentical subunits. *J. Bacteriol.*, **169**, 4124–4127.
27. Bassil,N., Maillart,E., Canva,M., Levy,Y., Millot,M.C., Pissard,S., Narwa,R. and Goossens,M. (2003) One hundred spots parallel monitoring of DNA interactions by SPR imaging of polymer-functionalized surfaces applied to the detection of cystic fibrosis mutations. *Sensors Actuators*, **94**, 313–323.
28. Bloch,V., Yang,Y., Margeat,E., Chavanieu,A., Auge,M.T., Robert,B., Arold,S., Rimsky,S. and Kochoyan,M. (2003) The H-NS dimerization domain defines a new fold contributing to DNA recognition. *Nat. Struct. Biol.*, **10**, 212–218.
29. Esposito,D., Petrovic,A., Harris,R., Ono,S., Eccleston,J.F., Mbabaali,A., Haq,I., Higgins,C.F., Hinton,J.C. *et al.* (2002) H-NS oligomerization domain structure reveals the mechanism for high order self-association of the intact protein. *J. Mol. Biol.*, **324**, 841–850.